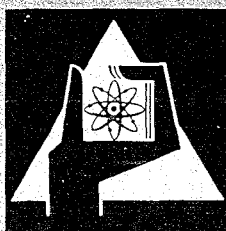# KERNFORSCHUNGSZENTRUM

KARLSRUHE

Mai 1969

Institut für Angewandte Kernphysik

Characteristics of Ion-Implanted Contacts for Nuclear Particle Detectors
I. Window Thickness of Ion-Implanted Semiconductor Detectors

O. Meyer

CHARACTERISTICS OF ION-IMPLANTED CONTACTS FOR NUCLEAR PARTICLE DETECTORS
I. Window thickness of ion-implanted semiconductor detectors

O. MEYER

Kernforschungszentrum Karlsruhe, Institut für Angewandte Kernphysik, Karlsruhe, Germany

The thickness of the entrance window of ion-implanted semiconductor counters was experimentally studied by pulse height defect measurements. It was found that the window thickness D strongly depends on the reverse voltage U_A. This dependence may be described by the function $U_A = F(D)^{-\eta}$. The influence of the following parameters on the constants F and η was measured: doping concentration of the base material, energy of the implanted ions, total number of implanted ions, annealing temperature, and crystal orientation. For boron-implanted contacts a formula is given that describes the measured results within 20%. Under certain conditions extremely thick windows up to 10 μm were found. In high resistivity material (100000 ohm·cm) for example thin windows ($< 0.02 \mu$m) require high reverse voltage (≈ 600 V); whereas in silicon with a resistivity smaller than 10000 ohm·cm, thin windows can easily be obtained even at small detector bias.

1. Introduction

Knowledge of the window thickness is most important for the spectroscopy of short range nuclear radiation. Measurements on diffused junction detectors[1] show the possibility to produce a minimum window thickness of 0.14 μm. For surface-barrier detectors[2] the window thickness was found to be a function of reverse voltage and doping concentration of the base material and may range between 0.01 and 0.2 μm.

In ion-implanted counters the window thickness is predominantly a function of the chosen ion energy and the angle between ion beam and crystal surface. In first measurements on boron-implanted contacts, produced with an ion energy of 5 keV, a window thickness of 0.2 μm was found[3]. For gallium contacts, implanted with an energy of 80 keV in germanium (the doping concentration of the contact was partially compensated by lithium) the window thickness was found to be between 0.3 and 0.8 μm [4].

The location of the p-n boundary ($N_A = N_D$) is determined by the tail of the distribution of the electrically active centers in the implanted contact[5]. This distribution in turn is determined by the energy loss mechanism, by crystal-lattice effects (crystal orientation and production of electrically active radiation defects) and by the substitution probability of implanted ions. Therefore the window thickness will further depend on the doping concentration of the base material, the ion mass and substitution probability, the annealing behaviour of electrically active defect centres and the channeling probability of implanted ions.

2. Experimental method

The window thickness or the dead layer of semiconductor detectors is defined as a surface layer which the charged particles have to cross before they reach the sensitive volume. In this dead layer the doping concentration is high and therefore there exists a high recombination probability. Charge carriers produced by ionisation in this dead layer do not participate in the charge collection and detection process. For determining the thickness of the entrance window, the reduction of α-particle pulse height, E', is measured as a function of the angle of incidence, θ. Here θ is the angle between crystal surface and α-particle beam direction[1]. Neglecting the energy loss in the evaporated contact layers the window thickness D is given by

$$D = E' / [(1/\sin\theta) - 1] (dE_0/dx)_{Si}.$$

dE_0/dx is 140 and 130 keV/μm for well-collimated α-particles from an ^{241}Am- and a ^{244}Cm-source, respectively[6,7]. For detector production n- and p-type silicon samples were used with resistivities of 7 000, 10 000, 20 000, 30 000, 80 000 and 100 000 ohm·cm. The samples are etched in CP$_4$ and immediately mounted in a target chamber. The implantation is performed in a liquid-air-trapped vacuum (8×10^{-6} Torr) within 2° parallel to the [111]-crystal axis[8]. The ion energy used is varied between 2 and 10 keV, the total ion number between 2.5×10^{11}/cm^2 and 10^{15}/cm^2. The window thickness is measured for both boron and tellurium implanted contacts. Besides, for comparison, other dopants were used, for example Bi, Sb, P, Li, Na, Ka and Cs. The samples were annealed in steps of 100° C up to 600° C (10 min at each step). During the annealing process molecular nitrogen was blown through the quartz tube for surface protection. Because of low dose implantation the surface resistance is often high. To

avoid rise time straggling thin (100–200 Å) contacts (Au and Al) were evaporated.

3. Experimental results

3.1. INFLUENCE OF DOPING CONCENTRATION OF THE BASE MATERIAL ON WINDOW THICKNESS

The values of the window thickness D measured as a function of the applied bias voltage for three boron-implanted samples (total ion number, $N = 10^{12}B^+/cm^2$ and ion-energy, $E = 4$ keV) with a donor concentration N_D of $6 \times 10^{10}/cm^3$, $2.5 \times 10^{11}/cm^3$, and $7 \times 10^{11}/$ $/cm^3$ are represented in fig. 1. In silicon with a specific resistivity up to 10 000 ohm·cm thin windows smaller than 0.02 μm can easily be obtained even at small detector bias. For high resistivity material (about 100 kohm·cm) thin windows require high reverse voltages (about 600 V). At low reverse voltage (< 10 V) and high resistivity material the window thickness is nearly independent of voltage and is about 10 μm thick. This measurement indicates that the depth of electrically active centers is 500 to 1000 times larger than the mean projected range for boron ions of that energy[5]. The result is only correct if the whole voltage drops at the p-n boundary and not at a possible series-resistance produced by a high resistivity layer in the implanted
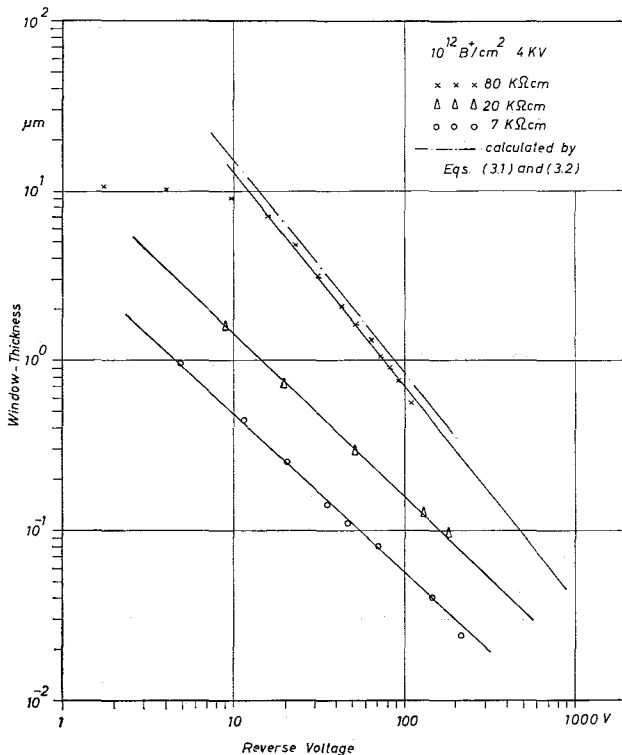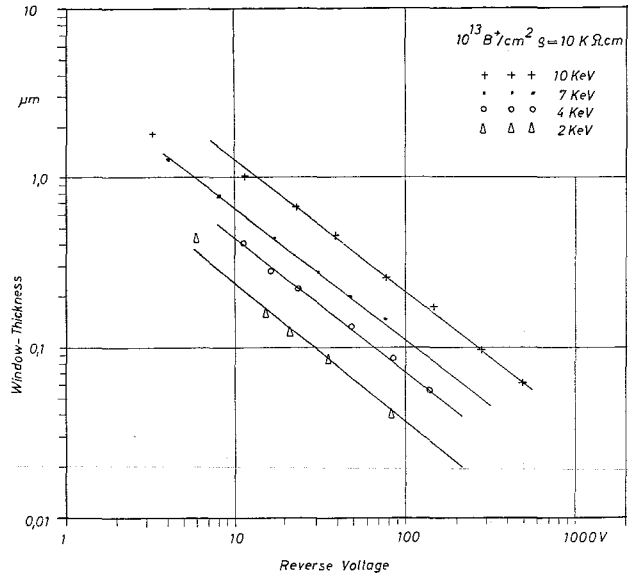

Fig. 2. Window thickness vs reverse voltage measured for different energies of implanted boron ions.

contact. The occurrence of such a resistance is ruled out by a measurement of the α-particle pulse height as a function of reverse voltage which shows that the maximum pulse height is reached at 5 V, independent of the resistivity of the base material. For all measurements log D decreases linear with log U_A. This behaviour may be described by $U_A = F(D)^{-\eta}$. The exponent η shows a small dependence of N_D.

3.2. INFLUENCE OF ION ENERGY ON WINDOW THICKNESS

Fig. 2 shows the results for boron-implanted contacts $(N = 10^{13}B^+/cm^2$, $N_D = 5 \times 10^{11}/cm^3)$, produced with ion energies of 2, 4, 7 and 10 keV. For the 2 keV-implanted contact a window thickness of 0.05 μm is reached at 60 V whereas for a 10 keV-implanted contact the same thickness is reached at 600 V. Analyzing the measured results one finds that the exponent η shows a small dependence on energy (η increases with energy) while F is energy dependent. For a high constant voltage U_0 the window thickness is proportional to the energy, in the low voltage range (< 10 V) a low-power dependence on the energy is found. Measurements at low voltage are often difficult to perform because of the bad energy resolution of the diodes in this voltage range.

3.3. INFLUENCE OF TOTAL NUMBER OF IMPLANTED IONS ON WINDOW THICKNESS

The measurements where performed on boron-implanted contacts (fig. 3a) produced on n-type silicon $(N_D = 2.5 \times 10^{11}/cm^3)$ with an ion energy of 4 keV and total ion numbers of $10^{12}/cm^2$ and $10^{15}/cm^2$. For the

Fig. 1. Window thickness vs reverse voltage measured for different doping concentrations of the base material.

high-dose-implanted contact the window thickness shows a weaker dependence on voltage than for the low-dose contact; at high voltages the window thickness is nearly independent of the voltage. On the other hand, low-dose-implanted contacts have a continuous decrease of window thickness up to high reverse voltages. The constants η and F are found to be:

Fig. 4. Influence of annealing temperature on window thickness, for a low-dose-implanted (a) and for a high-dose-implanted (b) boron contact.

$$\eta = 1.1 \text{ and } F = 2.78 \times 10^{-4} \ [\text{Vcm}^{-\eta}],$$
$$\text{for } 10^{12}\text{B}^+/\text{cm}^2,$$
$$\eta = 1.8 \text{ and } F = 5.07 \times 10^{-7} \ [\text{Vcm}^{-\eta}]$$
$$U_\text{A} > 40 \text{ V}: \ \eta = 4.5 \text{ and } F = 2.22 \times 10^{-18} \ [\text{Vcm}^{-\eta}]$$
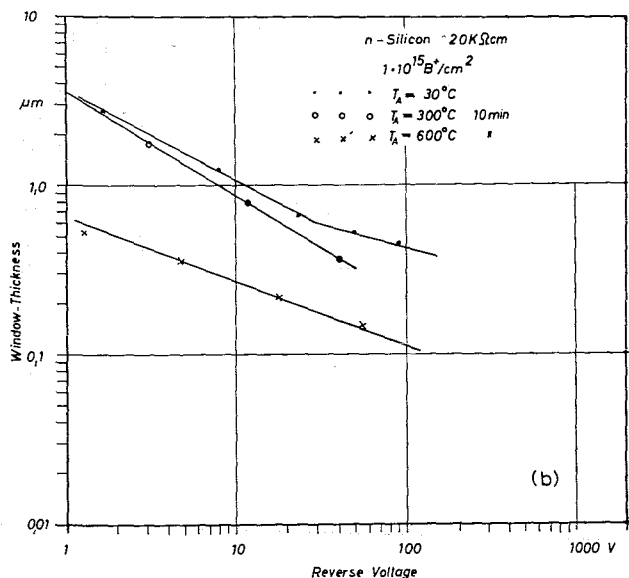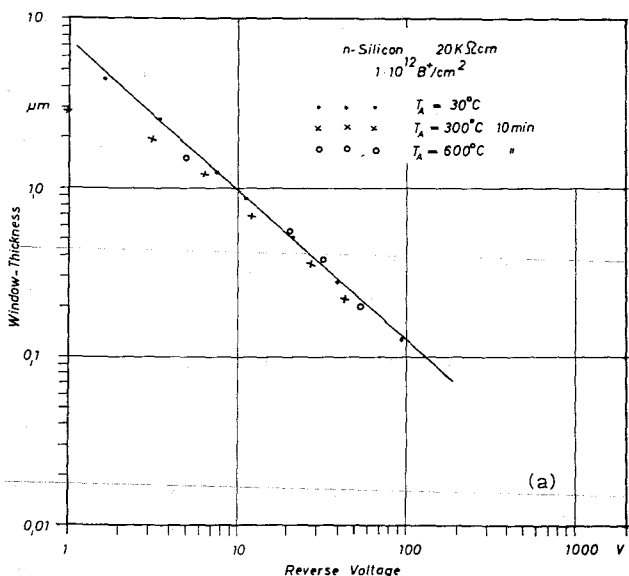$$\text{for } 10^{15}\text{B}^+/\text{cm}^2.$$

Fig. 3a. Window thickness vs reverse voltage measured for different total numbers of implanted boron ions.

Fig. 3b. Window thickness vs reverse voltage measured for different total numbers of implanted tellurium ions.
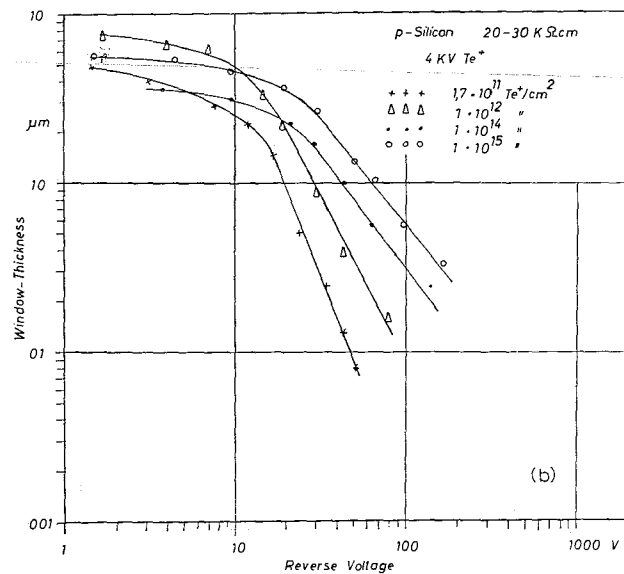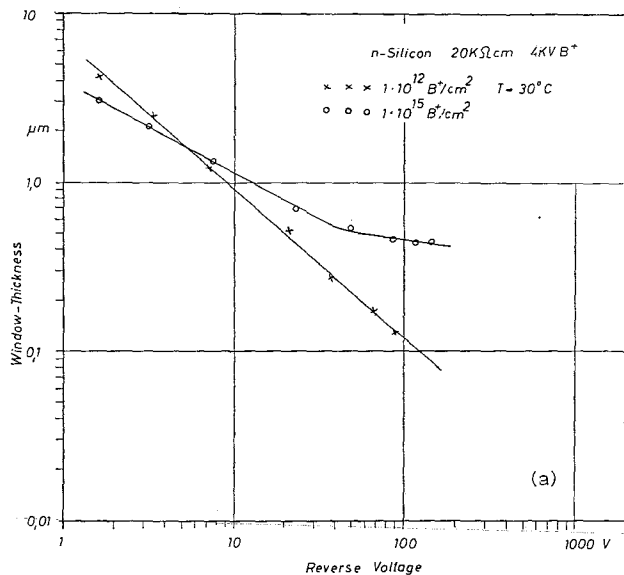
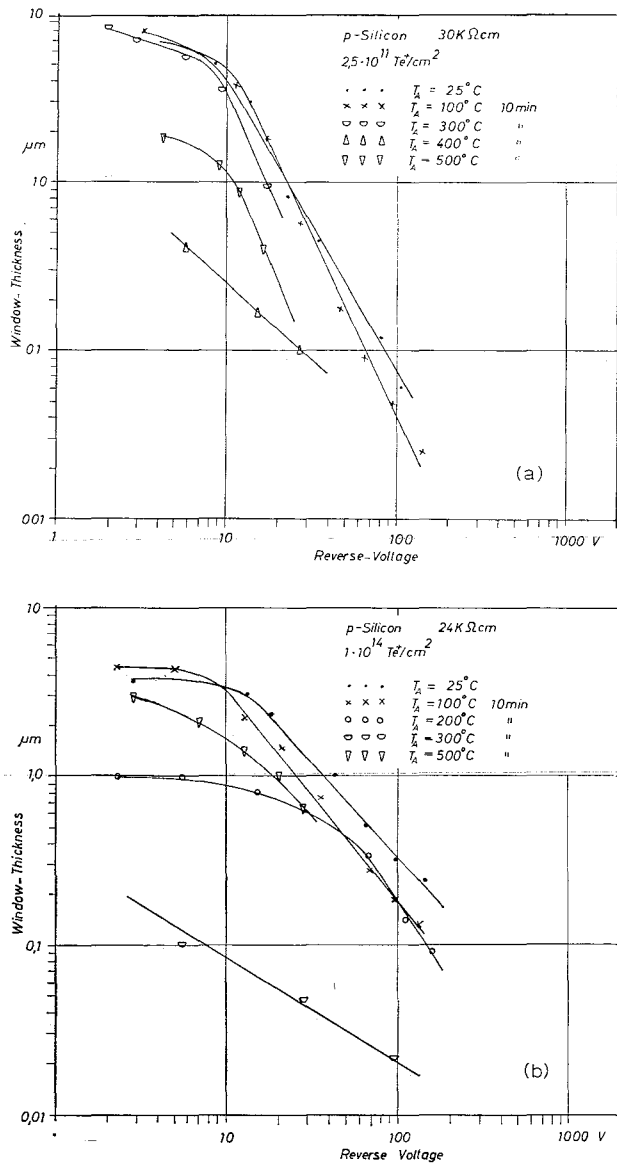The same measurements were done on tellurium-im-

Fig. 5. Influence of annealing temperature on window thickness, for a low-dose-implanted (a) and for a high-dose-implanted (b) tellurium contact.

planted contacts (fig. 3b), produced on p-type silicon ($N_A = 7-9 \times 10^{11}$/cm^3) with an ion energy of 4 keV and varying total ion numbers between 1.7×10^{11}Te$^+$/cm^2 and 10^{15}Te$^+$/cm^2. The measured profile is quite different compared with that of boron-implanted contacts: for low voltages (< 15 V) the window thickness is nearly constant, for higher voltages a steep decrease of window thickness is found depending on total ion number.

3.4. INFLUENCE OF ANNEALING TEMPERATURE ON WINDOW THICKNESS

Figs. 4a,b represent the measured voltage depen-

dence of the window thickness for low- and high-dose-implanted boron contacts (the implantation data are given in section 3.3) after annealing at 300, 500 and 600° C. For annealing temperatures up to 300° C there is only a small influence on both high- and low-dose-implanted contacts. For low-dose-implanted contacts the window thickness decreases in the low voltage range, for high-dose-implanted contacts in the high voltage range. Annealing temperatures above 500° C cause a strong decrease of window thickness over the whole voltage range for high-dose-implanted contacts; on the other hand the same temperatures have no influence on window thickness of low-dose-implanted contacts.

For tellurium-implanted contacts (figs. 5a,b) the influence of annealing temperature on the window thickness is different compared with boron-implanted contacts. At 200° C the window thickness decreases in the low voltage range for high-dose-implanted contacts. For annealing temperatures between 300 and 400° C a strong decrease of window thickness is found in both low- and high-dose-implanted contacts over the whole voltage range. For annealing temperatures greater than 500° C, the window thickness increases again very strongly.

3.5. INFLUENCE OF DIFFERENT DOPANTS AND ANNEALING TEMPERATURES ON THE WINDOW THICKNESS

The measurements have shown that for ion-implanted contacts a deep penetrating component exists probably caused by enhanced diffusion mechanisms[5]. For the production of ion-implanted semiconductor detectors it is of interest to know possibilities to avoid such a component. Therefore the voltage dependence of window thickness is measured for contacts produced with other dopants as a function of annealing temperature. The results are given in table 1, where the measured window thickness at a reverse voltage of 10 V is represented for different dopants and annealing tempera-

TABLE 1

Window thickness D (in μm), measured at 10 V reverse voltage for different dopants and annealing temperatures.

Substance	30° C	300° C	600° C
K	9	8.4	8.2
Cs	10.5	10	9.5
P	5.5	2	1
Sb	3.5	0.4	5
Bi	1.5	0.3	0.8
Te	10	0.6	3

tures. The used ion numbers were $10^{14}/cm^2$; the ion energy is 4 keV; the base material was p-type silicon with $\rho = 100\,000$ ohm·cm. The measured window thickness for interstitial donors (K and Cs) is about 10 μm and independent on annealing temperature. This result may arise from a preferential occupation of interstitial lattice sites during the implantation process. Thus the electrically active donor concentration is high compared with the concentration of active defect centers. Therefore annealing of defect centers has no effect on window thickness in this case. For phosphorous-implanted contacts there is a strong decrease of window thickness with increasing temperature. Antimony- and bismuth-implanted contacts show a similar behaviour as tellurium-implanted contacts. For annealing temperatures up to 300°C a strong decrease of window thickness is found, for temperatures greater than 500°C the window thickness increases again. This increase of window thickness is in agreement with the measured increase of charge carriers in antimony-implanted contacts for temperatures greater than 500°C[9]). Up to now it is not clear if this increase arises from annealing of active defect centers with acceptor behaviour or by a migration of dopants on substitutional lattice sites.

4. Emperical formula for the window thickness of boron-implanted contacts

For detector production it is necessary to know the window thickness D in advance. So the measurements were analysed quantitatively and the results are summarized in the following formulas:

$$D = \{F_0\rho^2 E^{1.3}/(NU_A)\}^{1/\eta}.$$

The constant F_0 is found to be $F_0 = 7 \times 10^5$

$$[Vcm^{\eta-2}/\{(kohm\cdot cm)^2 (keV)^{1.3}\}].$$

D[cm]   = window thickness;
ρ[kohm·cm] = specific resistivity of the base material;
E[keV]   = energy of implanted ions;
N[cm^{-2}]   = total number of implanted ions;
U_A[V]   = reverse voltage.

The exponent η is determined by the following formula:

$$\eta = \eta_0 N^{0.0767}/\rho^{0.0744},$$
$$\eta_0 = 0.147[(kohm\cdot cm)^{0.0744}/(cm^{-2})^{0.0767}].$$

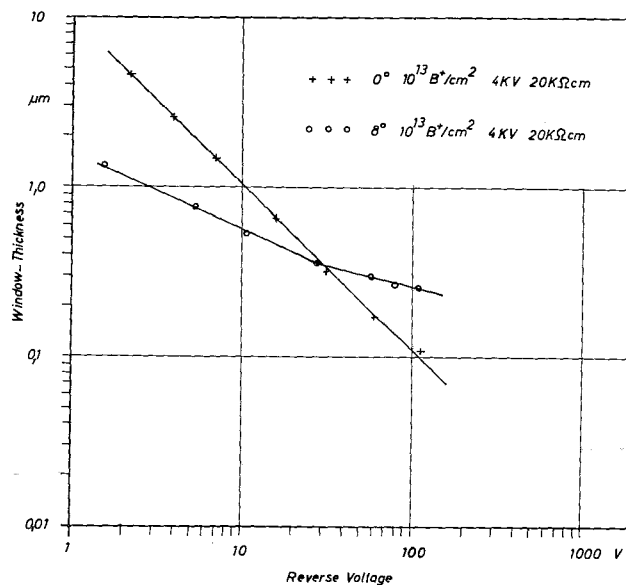The formulas (1) and (2) describe the measured results within $\pm 20\%$ for the following range of parameters:

Fig. 6. Window thickness vs reverse voltage measured for different crystal orientations.

$$T_A \leqq 300°C; \qquad U_A > 10\ V; \qquad 2 \leqq E \leqq 10;$$
$$1 \leqq \rho \leqq 100; \qquad 5 \times 10^{11} \leqq N \leqq 10^{15}.$$

As an example the following values of the parameters are used for calculation: $E = 4$ keV, $\rho = 80$ kohm·cm, and $N = 10^{12}/cm^2$; the calculated results are compared with measured values in fig. 1 (dashed line).

The formulas (1) and (2) are only valid for implantation within $\pm 2°$ parallel to the [111]-direction. Up to now the dependence of window thickness on the angle of incidence is not considered. The influence of this effect is represented in fig. 6. The window thickness for an 8° off-axis implantation is lower for low voltage and higher for high voltage compared to the window thickness of a well-collimated implantation. This result clearly shows that the channeling probability for off-axis implantation is diminished, on the other hand for low penetration depth the doping probability is higher partially by enhanced electrically active defect production. Quantitative conclusions are not drawn from this measurement because an accidental implantation in higher index crystallographic directions or in crystal-planes could not be excluded.

References

[1]) R. L. Williams and P. P. Webb, IRE Trans. NS-9, no. 3 (1962) 160.
[2]) G. Forcinal, P. Siffert and A. Coche, IEEE Trans. NS-15, no. 3 (1968) 275.
[3]) S. Kalbitzer et al., Z. Physik 203 (1967) 117.
[4]) R. Ellis, Grenoble (1967) Conf. *Applications of ion beams to semiconductor technology* (ed. P. Glotin; Centre d'Etudes Nucléaire).
[5]) J. W. Mayer and O. J. Marsh, *Applied Solid State Science* 1 (Academic Press, N.Y., 1968).
[6]) W. Whaling, *Handbuch der Physik* 34 (1958) p. 153.
[7]) H. Kobayashi and S. Konno, Phys. Chem. Res. Jap. 57 (1963) 144.
[8]) O. Meyer, IEEE Trans. NS-15, no. 3 (1968) 232.
[9]) J. W. Mayer et. al., Can. J. Phys. 45 (1967) 4073.

CHARACTERISTICS OF ION-IMPLANTED CONTACTS FOR NUCLEAR PARTICLE DETECTORS

II. Concentration distribution in ion-implanted contacts for semiconductor detectors

O. MEYER

Kernforschungszentrum Karlsruhe, Institut für Angewandte Kernphysik, Karlsruhe, Germany

An analytical treatment is given which allows the calculation of the depth concentration of electrically active centers in ion-implanted contacts, starting from the measured dependence of the window thickness on reverse voltage. The influence of the following parameters on the depth distribution is studied: dopants, ion energy, ion concentration, doping concentration of the base material, crystal orientation, and annealing temperature. By variation of the doping concentration of the base material it is possible to determine the concentration distribution over four orders of magnitude. The minimum detectable concentration is about 10^{12}/cm^3. The results are related to other observations obtained in measuring concentrations profiles by different methods.

1. Introduction

Methods for measuring density profiles may roughly be divided into two groups:

a. Techniques for layer removal of well-known thicknesses as for example anodic oxidation and dissolution of the oxide in HF;

b. Nondestructive measurement techniques.

Radio tracer techniques and Hall-effect together with sheet resistivity measurements belong to the first group. Activity measurements yield the total number of implanted radionucleides. The concentration distribution is measured over 3 to 4 orders of magnitude down from the maximum value[1,2]. The electrical characteristics of implanted contacts can be obtained from Hall and resistivity measurements[3].

Nondestructive measurement techniques are the capacitance-voltage method[4] and the window thickness-voltage method, discussed in this paper. With these methods it is possible to measure the concentration of electrically active centers down to the doping concentration of the used base material.

The results of these experiments have indicated that a deep penetration component exists for ion implanted contacts in silicon. With radio tracer techniques a deep penetration tail was found in tungsten[5] but not in silicon[2]. Therefore it is assumed that the deep penetration component consists of fast diffusing electrically active defect centers. Measurements are in progress to confirm this assumption.

2. Calculation of concentration distribution from voltage dependence of window thickness

In the preceding paper[6] it was shown that it is possible to describe the measured voltage dependence of the window thickness D by the function

$$U_A = F(D)^{-\eta}. \qquad (1)$$

This formula is valid for a certain range of reverse voltages. Deviations from experimental results are
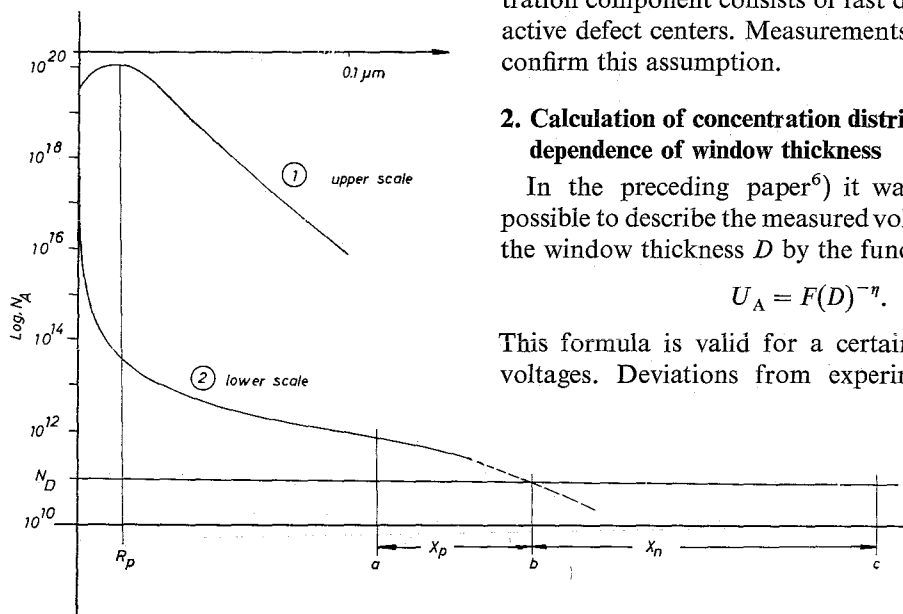

Fig. 1. Schematic drawing of the concentration distribution of electrically active centers for a boron-implanted contact in high resistivity n-type silicon. In curve 1 the distance scale is enlarged for clearence. Curve 2 represents the measured results in linear distance scale, point *b* is about 10 μm.

found in the high and low voltage range. In the low voltage range the measured window thickness is often smaller, in the high voltage range in a few cases greater than the window thickness predicted by formula (1). In the high voltage range the deviation can be described by an additional constant D_0 as $U_A = F(D_0+D)^{-\eta}$. In most cases D_0 is small compared with D and is therefore neglected. The constants F and η were found to depend on a number of parameters such as ion energy, total ion number, doping concentration of the base material, annealing temperature, and others.

The schematic drawing (fig. 1) represents the depth distribution of acceptors $N_A(x)$, for example for an implanted boron contact, in high-resistivity n-type material with the doping concentration N_D of the base material. Point b marks the location of the p-n boundary $N_A(b)=N_D$. In curve 1 the distance scale is enlarged for elucidation. Curve 2 represents the measured results (section 3.1) for boron implanted contacts in a linear distance scale, point b is about 10 μm. The sensitive region in the n-type material is $x_n = c - b$; $x_p = b-a$ is the sensitive region in the p-type material. The window thickness D is defined as the distance between zero and the voltage dependent boundary a, in other words $D = a$. The constant D_0 may be identified with the mean projected range R_p ($R_p = 50 - 300$ Å for the implantation energy used). Even at high voltage boundary a was found to be large compared with R_p.

The reverse voltage U_A drops across the sensitive region $c - a$. A variation of U_A by ΔU_A will change a by Δa and c by Δc. From the Poisson equation it follows that the derivative of the field strength at a and c is proportional to the doping concentration there. The electric potential difference U_A across $c - a$ may be expressed by

$$U_A = \int_a^c E(x)\,dx, \qquad (2)$$

where $E(x)$ is given by

$$E(x) = E(a) + \int_a^x \{dE(y)/dy\}\,dy. \qquad (3)$$

From charge neutrality outside the depletion layer follows: $E(a) = 0$. The fixed space charges in the depletion layer will be governed by the Poisson equation:

$$dE(x)/dx = \{q/(\varepsilon\varepsilon_0)\}\{N_A(x)-N_D\}. \qquad (4)$$

The neutrality condition for a p-n junction is expressed by

$$\int_a^c \{N_A(x)-N_D\}\,dx = 0. \qquad (5)$$

From eqs. (2) and (5) we get

$$U_A = \{-q/(\varepsilon\varepsilon_0)\}\int_a^c\int_x^a \{N_A(y)-N_D\}\,dy\,dx. \qquad (6)$$

From measurements of the capacitance as a function of U_A the following relation is found:

$$c - a = \delta U_A^{\frac{1}{4}}, \text{ for } U_A > 5 \text{ V and } \delta^2 = 2\varepsilon\varepsilon_0/(qN_D). \qquad (7)$$

For the concentration distribution $N_A(x)$ of the electrically active centers in ion implanted contacts we assume the form

$$N_A(x) = K(x)^{-n}; \qquad K = N_D b^n. \qquad (8)$$

This assumption is tested by inserting eq. (8) in eqs. (5) and (6). From eq. (6) we get

$$U_A = \{qN_D/(\varepsilon\varepsilon_0)\}[\{b^n(c^{2-n}-a^{2-n})\}/\{(1-n)(2-n)\} - \{a^{1-n}b^n/(1-n)\}(c-a)-\tfrac{1}{2}(c-a)^2]. \qquad (9)$$

Eq. (5) yields

$$\{b^n/(1-n)\}(c^{1-n}-a^{1-n})-(c-a) = 0. \qquad (10)$$

If the approximation $a \ll c$ is used, we get from eq. (10):

$$b^n/(1-n) = c/(c^{1-n}-a^{1-n}). \qquad (11)$$

Eq. (11) inserted in eq. (9) shows that the assumption of eq. (8) holds only if the following conditions are fulfilled:

$$|(c/a)^{2-n}-1| \ll |\tfrac{1}{2}(2-n)c/a|, \qquad (12)$$

$$c^{1-n} \ll a^{1-n}. \qquad (13)$$

Eq. (12) is also valid for $n = 2$; using de l'Hôpital's theorem we get:

$$|\ln(a/c)| \ll \tfrac{1}{2}+\tfrac{1}{2}(c/a).$$

If the conditions (12) and (13) are valid, U_A can be eliminated from eq. (9) since the first term is negligible. Then the potential difference U_A as a function of boundary a is found to be

$$U_A = [qK^2/\{2\varepsilon\varepsilon_0 N_D(1-n)^2\}]a^{2-2n}. \qquad (14)$$

Comparing eq. (13) with the experimental result given in eq. (1) it is found:

$$-\eta = 2-2n; \qquad F = qK^2/\{2\varepsilon\varepsilon_0 N_D(1-n)^2\}. \qquad (15)$$

Thus the concentration distribution of eq. (8) is completely determined. A careful evaluation is necessary, in what range of boundary a the conditions (12) and (13) are valid. With $a \ll c$ and $n \geq 1.3$ ($1.3 < n < 3.2$ is experimentally verified), eq. (13) can easily be fulfilled. A minimum reverse voltage U_{A_0} is defined were the ratio of the terms in eq. (12) is at least 1:10. For U_{A_0} the corresponding values of a and c are called a_0 and c_0,

respectively. If the reverse voltage increases (a decreases and c increases) the ratio (12) becomes smaller because $2 - n < 1$. Values of U_{A_0}, a_0, and c_0 have been included in tables 1, 2 and 3. In some cases where the condition (12) is not well fulfilled the ratio of the terms is given in the table. The concentration distribution derived from the data is valid for parameter a within the interval $D_0 < a \leqq a_0$.

3. Results of the analysis

3.1. DOPING CONCENTRATION OF THE BASE MATERIAL

The measurements presented in [6]), section 3.1 were analysed by means of eq. (1). The constants n and K are then calculated by eq. (15). The results of this analysis are given in table 1.

Fig. 2 represents the concentration distribution of electrically active centers for boron-implanted contacts at room temperature. The profile is determined over nearly 3 orders of magnitude between about 1% and 0.001% of the concentration maximum. The dashed curve corresponds to values of the terms in eq. (12) which yield ratios less favourable. The profile given by the dashed-dotted line down to $6 \times 10^{10}/cm^3$ has been estimated from the measured data.

3.2. INFLUENCE OF TOTAL NUMBER OF IMPLANTED IONS ON CONCENTRATION DISTRIBUTION

The measurements which are given in [6]), section 3.3 were analysed. The results of the calculation are represented in table 2.

The concentration distributions for boron-implanted contacts at room temperature are monotonously decreasing functions of the depth down to a concentration of $10^{12}/cm^3$ (fig. 3, curves 1 and 2). For high dose implanted contacts the slope is steeper than for low dose contacts. The concentration profile for high dose contacts shows a steep increase for small penetration depths. Comparing the absolute values of concentration for high and low dose implantation one finds that for deep penetration depth the doping probability depends on the total number of implanted boron ions: an increase of
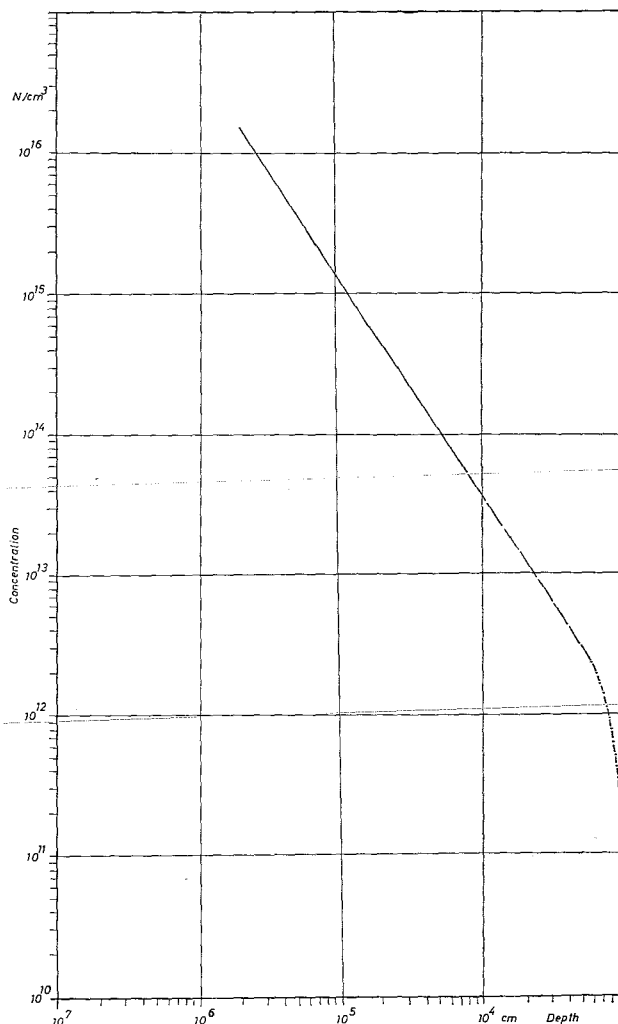

Fig. 2. Concentration distribution of electrically active centers in a boron-implanted contact.

the total number from $10^{12}/cm^2$ to $10^{15}/cm^2$ produces the same or even a smaller concentration of electrically active centers. High dose implantation will produce a highly damaged region at the crystal surface which

TABLE 1
Influence of the doping concentration of the base material on concentration distribution.
Calculated values for the constants K and n.
$N = 10^{12}/cm^2$; $E_{B+} = 4$ keV; $T_A = 300°$K.

N_D (cm^{-3})	η	F (Vcm^{-n})	n	K (cm^{n-3})	U_{A_0} (V)	a_0 (μm)	c_0 (μm)
6×10^{10}	0.84	3.5×10^{-2}	1.42	6.3×10^7	100	0.7	1.500
2.5×10^{11}	1.02	1.29×10^{-3}	1.51	2.4×10^7	30	0.5	400
7×10^{11}	1.07	2.63×10^{-4}	1.53	2.83×10^7	20	0.25	200

TABLE 2
Influence of the total number of implanted ions on concentration distribution.
Calculated values for the constants K and n.
$E(B^+,Te^+) = 4$ keV; $\rho_n = 20$ kΩ cm; $\rho_p = 20$–30 kΩcm; $T_A = 300°$K.

Dopant	Total number	η	F (Vcm$^{-\eta}$)	n	K (cm^{n-3})	U_{A_0} (V)	a_0 (μm)	c_0 (μm)
B$^+$	10^{12}/cm^2	1.1	2.78×10^{-4}	1.55	1.83×10^7	20	0.5	320
	$U_A < 40$ V: 10^{15}/cm^2	1.8	5.08×10^{-7}	1.9	1.16×10^6	5	1.6	160
	$U_A > 40$ V: 10^{15}/cm^2	4.5	2.2×10^{-18}	3.25	6.1	< 1	–	–
Te$^+$	1.7×10^{11}/cm^2	0.37	0.67	1.18	4.6×10^8	ratio is about 1:2 at 50 V		
	10^{12}/cm^2	0.516	0.25	1.26				
	10^{14}/cm^2	0.736	4.94×10^{-2}	1.36				
	10^{15}/cm^2	0.827	3.16×10^{-2}	1.42	2.38×10^8	ratio is about 1:6 at 100 V		

reduces the probability for a deep penetrating component[2].

The concentration distribution in tellurium contacts implanted at room temperature (curves 3 and 4 in fig. 3) has a smaller slope compared with boron-implanted contacts and a steep decrease is found for deep penetra- tion depths (dashed lines). In contrast to boron-im- planted contacts the concentration increases with in- creasing total ion number even at deep penetration depths. An increase of the total ion number by a factor 5000 causes the concentration to increase by a factor 3 deep depths and a factor 7 for small depths.
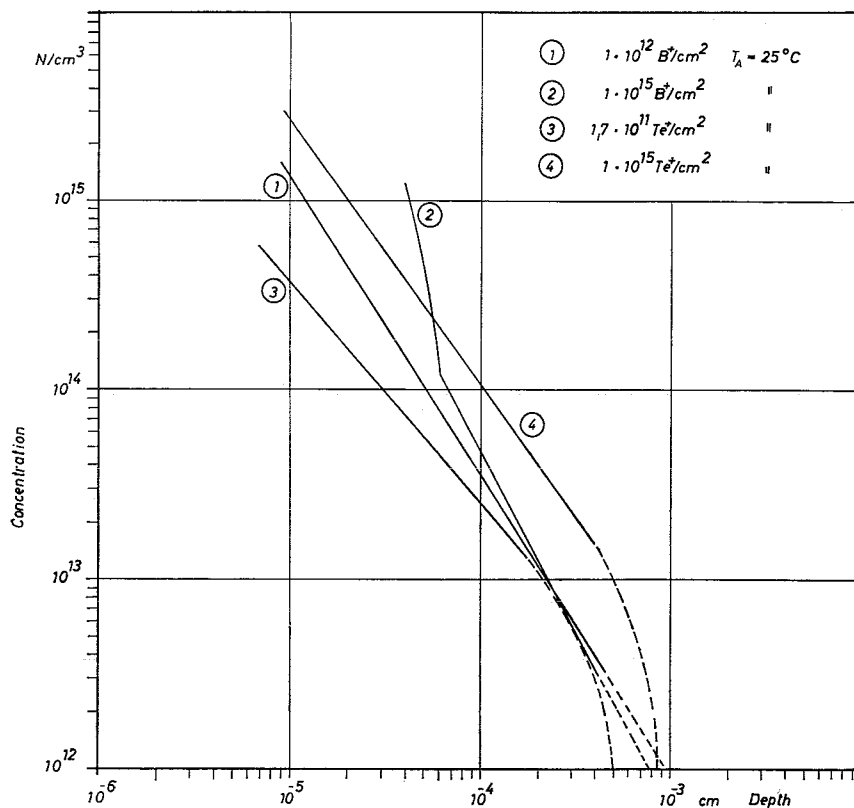

Fig. 3. Concentration distribution of electrically active centers in boron and tellurium high and low dose implanted contacts.

TABLE 3
Influence of annealing temperature on concentration distribution.
Calculated values for the constants K and n.
$E(\mathrm{B^+,Te^+}) = 4$ keV; $\rho_n = 10$ kΩcm; $\rho_p = 24$ kΩcm.

Dopants	T_A (C°)	Total number	η	F (Vcm$^{-\eta}$)	n	K (cm^{n-3})	U_{A_0} (V)	a_0 (μm)	c_0 (μm)
B$^+$	30	10^{15}/cm^2	1.83	5.1×10^{-7}	1.91	1.16×10^6	<1	–	–
	500	10^{15}/cm^2	2.69	4.7×10^{-12}	2.34	3.54×10^3	<1	–	–
Te$^+$	30	10^{14}/cm^2	0.88	1.2×10^{-2}	1.44	1.45×10^8	ratio is about 1:5 at 50 V		
	300	10^{14}/cm^2	1.6	7.5×10^{-8}	1.8	5×10^5	2	0.23	70

3.3. INFLUENCE OF ANNEALING TEMPERATURE ON CONCENTRATION DISTRIBUTION OF IMPLANTED IONS

The measurements for high dose implanted boron and tellurium contacts presented in [6]), section 3.4, were analysed. The results are given in table 3.

The calculated concentration distributions are shown in fig. 4. By comparison of curves 1 and 2 for high dose implanted boron contacts at 30 and 300°C it is found that annealing strongly reduces the concentration over the whole range of penetration depth. The steep increase of concentration at low penetration depth for room temperature implanted boron contacts has completely disappeared. The slope of curve 2 is steeper ($n = 2.34$) than the slope of curve 1 ($n = 1.9$). From this result it is concluded that the annealing effect is more pronounced at deep penetration depths. For low dose implanted boron contacts [fig. 4a in [6]), data not quantitatively analysed] an annealing effect is only found for

Legend:
① $1 \cdot 10^{15}$ B$^+$/cm^2 $T_A = 30°C$
② $1 \cdot 10^{15}$ B$^+$/cm^2 $T_A = 500°C$ 10min
③ $1 \cdot 10^{14}$ Te$^+$/cm^2 $T_A = 30°C$
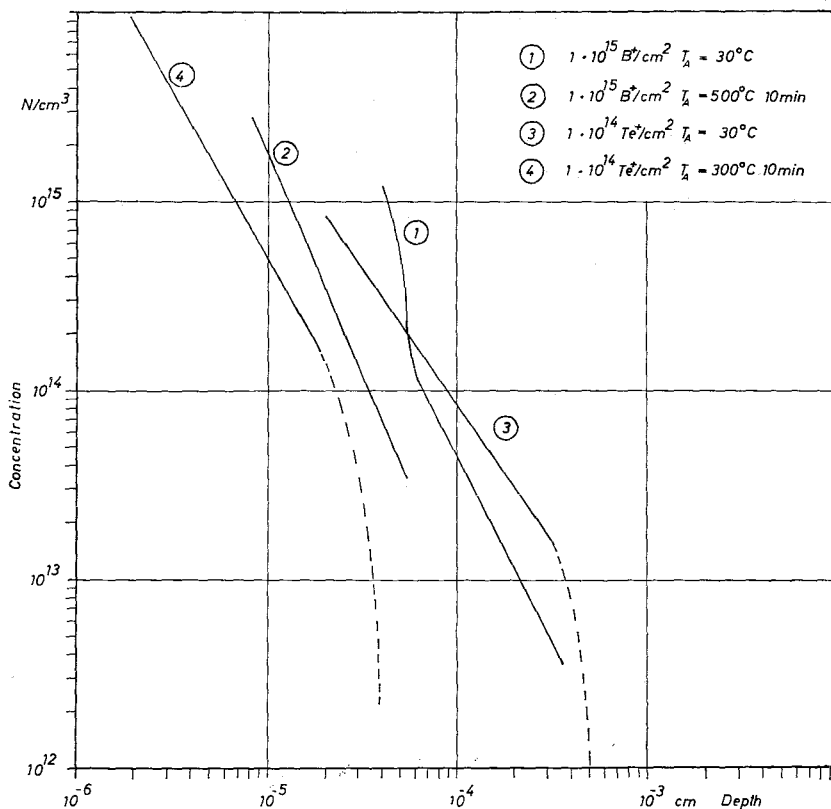④ $1 \cdot 10^{14}$ Te$^+$/cm^2 $T_A = 300°C$ 10min

Fig. 4. Concentration distribution of electrically active centers in high dose boron and tellurium contacts for different annealing temperatures.

deep penetration depths. Thus for low dose implantation the production of active radiation defects is low. On the other hand, the annealing effect found for the deep penetration component again is a hint that the tail consists mostly of electrically active defect centers. By comparison of curve 1 in fig. 3 (only the deep penetration tail decreases at 500° C) and curve 2 in fig. 4 it is concluded that in low dose implanted boron contacts even the subsitution probability is higher than in high dose implanted boron contacts.

Curves 3 and 4 in fig. 4 show the concentration profile in high dose implanted tellurium contacts. Again the slope for the annealed contacts at 300° C is steeper than the slope for unannealed contacts, in additon the strong annealing effect for the deep penetration tail is obvious. The steep increase of window thickness [fig. 5a, b in [6]) found at high annealing temperatures (500° C) in tellurium, antimony, and bismuth implanted contacts is in agreement with the measured increase of charge carrier concentration for antimony implanted contacts[3])].

4. Discussion

The deep penetration tail which is found for different dopants implanted in high resistivity n- and p-type silicon is probably due to a fast diffusing component of electrically active centers. Measurements on ionisation and activation energies are in progress to verify this assumption.

The concentration profile for deep penetration depth does not increase with increasing total ion number and decreases with increasing annealing temperature. After annealing the absolute value of concentration is lower for high dose than for low dose implanted boron con-

tacts. From this result it is assumed that the substitution probability is higher for low dose implantation, at least for boron ions. For off-angle implantations[6]) the concentration is reduced at deep penetration depths. For both high and low dose tellurium contacts there is an increase in concentration at annealing temperatures between 500 and 600° C, the same increase is found for antimony- implanted contacts.

The analytical treatment presented in section 2 holds for exponents $n > 1.6$. For smaller exponents (especially for tellurium contacts implanted at room temperature) the condition (12) is fulfilled only in the high voltage range.

From a theoretical point of view there are many possibilities of obtaining power-law concentration distributions of implanted ions and of other "damage centers" in supertails[7]). Up to now a careful comparison between theory and experiment has not yet been performed.

References

[1] J. A. Davies, F. Brown and M. McCargo, Can. J. Phys. 41 (1963) 829.
[2] G. Dearnaley et al., Can. J. Phys. 46 (1968) 587.
[3] J. W. Mayer et al., Can. J. Phys. 45 (1967) 4073.
[4] R. W. Bower et al., Appl. Phys. Lett. 9 (1966) 203.
[5] J. A. Davies and P. Jespersgard, Can. J. Phys. 44 (1966) 1631.
[6] O. Meyer, Nucl. Instr. and Meth. 70 (1969) 279.
[7] M. Sparks, Phys. Rev. Lett. 17 (1966) 1247; private communication.